Journal of Structural Biology 166 (2009) 272–287

Contents lists available at ScienceDirect

Journal of Structural Biology

journal homepage: www.elsevier.com/locate/yjsbi

Br-rich tips of calcified crab claws are less hard but more fracture resistant: A comparison of mineralized and heavy-element biological materials

Robert M.S. Schofield [a,*], Jack C. Niedbala [a], Michael H. Nesson [b], Ye Tao [c], Jacob E. Shokes [d], Robert A. Scott [d,e], Matthew J. Latimer [f]

[a] Department of Physics, University of Oregon, 1274, Eugene, OR 97403, USA
[b] Department of Biochemistry and Biophysics, Oregon State University, Corvallis, OR 97331, USA
[c] Beijing Synchrotron Radiation Facility, Institute of High Energy Physics, Chinese Academy of Sciences, Beijing 100049, China
[d] Department of Chemistry, University of Georgia, Athens, GA 30602, USA
[e] Department of Biochemistry and Molecular Biology, University of Georgia, Athens, GA 30602, USA
[f] Stanford Synchrotron Radiation Lightsource, SLAC National Accelerator Laboratory, Menlo Park, CA 94025, USA

ARTICLE INFO

Article history:
Received 10 November 2008
Received in revised form 19 January 2009
Accepted 22 January 2009
Available online 4 February 2009

Keywords:
Crab
Cheliped
Biomineralization
Bromine
Zinc
Br
Zn
Mechanical properties
Hardness
Modulus of elasticity
Metal
Halogen
Abrasion
Energy of fracture
XAS
Bromotyrosine
Arthropod
Cuticle
Exoskeleton
Invertebrate
Scanning X-ray microscopy
Scanning X-ray microprobe spectroscopy
EXAFS

ABSTRACT

We find that the spoon-like tips of the chelipeds (large claws) of the crab *Pachygrapsus crassipes* differ from the rest of the claw in that they are not calcified, but instead contain about 1% bromine—thus they represent a new example of a class of structural biological materials that contain heavy elements such as Zn, Mn, Fe, Cu, and Br bound in an organic matrix. X-ray absorption spectroscopy data suggest that the bromine is bound to phenyl rings, possibly in tyrosine. We measure a broad array of mechanical properties of a heavy-element biological material for the first time (abrasion resistance, coefficient of kinetic friction, energy of fracture, hardness, modulus of elasticity and dynamic mechanical properties), and we make a direct comparison with a mineralized tissue. Our results suggest that the greatest advantage of bromine-rich cuticle over calcified cuticle is resistance to fracture (the energy of fracture is about an order of magnitude greater than for calcified cuticle). The greatest advantage relative to unenriched cuticle, represented by ant mandible cuticle, is a factor of about 1.5 greater hardness and modulus of elasticity. The spoon-like tips gain additional fracture resistance from the orientation of the constituent laminae and from the viscoelasticity of the material. We suggest that fracture resistance is of greater importance in smaller organisms, and we speculate that one function of heavy elements in structural biological materials is to reduce molecular resonant frequencies and thereby increase absorption of energy from impacts.

1. Introduction

Invertebrates modify their mechanical structures with a variety of inorganic materials, often employing multiple modification systems in close proximity (Schofield, 2001). The possibility that different systems of inorganic elements are used in imparting different balances of mechanical properties seems likely, but has not been explored. Here we show that, in addition to calcification, certain crabs employ a bromine-rich biological material in the tips of cuticular structures, and we study the different mechanical properties associated with calcified, brominated and unenriched cuticle. Bromine is one of a variety of heavy elements including zinc, iron, copper and manganese, that are employed by invertebrates in concentrations ranging between 1% and 25% of dry mass in mandibular teeth, tarsal (leg) claws, stings and other "tools"

* Corresponding author.
E-mail address: rmss@conch.uoregon.edu (R.M.S. Schofield).

1047-8477/$ - see front matter © 2009 Elsevier Inc. All rights reserved.
doi:10.1016/j.jsb.2009.01.007

(Schofield, 2001). These heavy-element biological materials differ from calcified cuticle in that a separate mineral phase is not evident (Schofield et al., 2003). Furthermore, the concentration of the metal or halogen is usually lower than that of calcium in calcified cuticle. Nevertheless, heavy-element-modified materials possess markedly different mechanical properties from those of unmodified materials. For example, we have found that the hardness of the mandibular teeth of leaf-cutting ants increases nearly threefold as zinc (reaching 16% of dry mass) is incorporated during early adult life (Schofield et al., 2002). A similar hardness variation with zinc content was observed in zinc removal and replacement experiments in nereid worm jaws (Broomell et al., 2006). But the differences in a broad range of mechanical properties of the differently modified cuticles have not been examined. Since some crustaceans employ both calcified and bromine-enriched cuticle, they represent a good system for comparing mineralized and heavy-element biological materials.

The chelipeds (large claws) of certain crabs have a spoon-like tip (Warner, 1977). In some species these spoon tips appear to differ in composition from the rest of the claw in that they are darker and translucent and thus appear not to be calcified (see Fig. 1a).

We have observed these distinct spoon-like tips in a variety of crabs, including members of the Grapsidae (shore crabs) and Gecarcinidae (land crabs), as well as anomurans such as members of Lithodidae (stone and rock crabs), Paguridae (right handed hermit crabs, often evident only on the small claws), and Coenobitidae (land hermit crabs).

Pachygrapsus crassipes is an omnivorous crab; individuals scavenge and graze on algae such as *Ulva*, and they attack and eat other crabs and living fish (Bovbjerg, 1960). In the laboratory, we have observed the spoon tips being used as spoons, to carry snail eggs to the crab's mouthparts, and as clamps, with the articulating surfaces of opposing spoon tips gripping sheets of the alga *Ulva* (this was done with both chelipeds to tear apart the alga for consumption). We have observed similar gripping and tearing of prey material, such as other crab legs. We have also observed the spoon tips being used as forceps, picking bits of tissue from inside crab prey, and picking bits of algae from between barnacles on rocks. Finally, we have observed that the spoon tips have pierced the calcified cuticle of other crabs.

The translucent Br-rich cuticle forming the spoon tips of these claws is similar to material at the tips of the walking legs of many crabs, including crabs that do not have the spoon-like features at the cheliped tips. For example, the tips of the chelipeds of the Dungeness crab, *Cancer magister*, are calcified, but the walking legs are tipped with translucent material that extends in vertical strips a centimeter or so up the dactylus, an arrangement that increases the interface area and may thereby reduce the likelihood that the tip will break off at the interface. The uncalcified material at the tips of the walking legs of crabs has been found to be bromine-rich in the examined specimens (Schofield, 1990, 2001, this work).

It is important to distinguish the relatively dark but translucent material studied here from the regions of dark opaque pigmentation on the distal portions of many crab claws such as members of the *Cancer* genus and the stone crab *Menippe mercenaria*. The material we study here appears to be a separate structure at the tip of the claw—distinguished by its translucence. In contrast, the darkly pigmented regions on other claws often cover a large portion of the fingers of the claw and consist of a thin layer that often wears away, leaving white regions at the contact surfaces of the claw teeth.

Previous studies related to the mechanical properties of crab claws have focused on these darkly pigmented claws and claws that are designed for crushing, rather than claws with spoon tips. The pigmented region of the fingers of stone crabs were found to be harder and more resistant to fracture (Melnick et al., 1996), and the authors hypothesized that this was due either to the lower porosity of the distal portions of the claw or else to the dark pigmented layer.

Several studies have noted the prevalence of claw wear and breakage in wild populations of crabs, and have suggested that damage to the claws is likely to reduce crab fitness. Juanes and Hartwick (1990) found that Dungeness crabs (*C. magister*) with claw teeth that had been filed down to match the approximate level of wear found in 25% of wild "mated" males, spent significantly longer times breaking clams than did those with untreated claw teeth. Other authors have also noted that crabs with broken or worn claws have a greater difficulty breaking open mollusks in the lab (Juanes and Hartwick, 1990; Behrens Yamada and Boulding, 1998). In addition to reducing feeding efficiency, wear and damage may also interfere with fighting and reproductive success (Juanes and Hartwick, 1990). In a separate investigation, about 6% of crabs from six different *Cancer* species had broken claws (Palmer et al., 1999; Taylor et al., 2000), mainly broken claw tips.

A number of authors have suggested that crabs modify their behavior to reduce the probability of damage to their claws. The avoidance of claw damage may explain observations such as prey selection that is not optimal for energy gain and declining muscle stress with claw size (Juanes and Hartwick, 1990; Seed and Hughes, 1995; Palmer et al., 1999; Taylor, 2001; Smallegange and Van Der Meer, 2003).

Although these studies focus on claws designed for crushing, they demonstrate that fracture and wear of calcified claw cuticle can be important problems, and demonstrate that these tools can be operating close to their mechanical limits.

Bromine, in concentrations reaching percent levels, has been reported in structural tissues of a wide variety of mainly marine organisms, including annelid worm jaws (Bryan and Gibbs, 1979), crab tarsal claws, marine and terrestrial isopods, horseshoe crabs (Schofield, 1990), corals (Goldberg et al., 1994), pycnogonids (Schofield, 2001) and priapulids (this work). In some cases, chlorine and iodine are found along with bromine. Brominated tyrosine

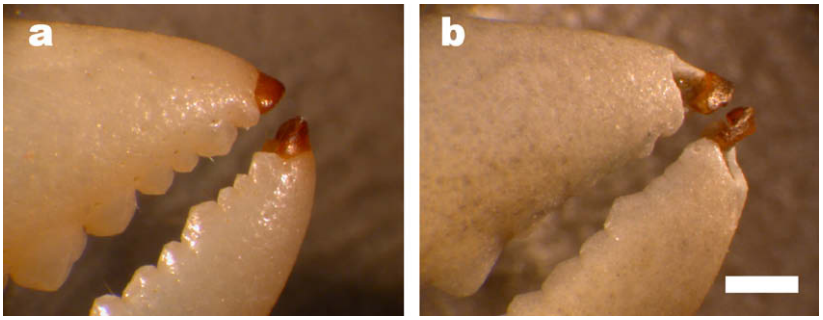

Fig. 1. The tips of the chelipeds (claws) of a crab, *Pachygrapsus crassipes*, before (a) and after (b) bead blasting. The bromine-rich material is the darker material at the tip of the claws. The claw tips are less eroded by the bead blasting than surrounding calcified material, suggesting a greater resistance to chipping from impact. Scale bar: 2 mm.

derivatives have been reported in sponges and gorgonian corals (Low, 1951; Roche, 1952), the operculae of whelks (Hunt and Breuer, 1971), the cuticle of horseshoe crabs (Welinder, 1972) and polychaete worm jaws (Birkedal et al., 2006). While some authors have suggested that halogenated phenyl rings are an incidental byproduct of sclerotization in sea water, Pryor (1962) suggested a functional role for halogenated tyrosine derivatives: that the electrophilic halogens would generate a partial positive charge on the phenolic hydroxyl groups which might then participate in cross-linking proteins. The suggestion that halogenation is a non-functional byproduct of sclerotization in sea water is contradicted by the presence of bromine in tarsal claws of land-based crustaceans, such as isopods (Schofield, 2001). A functional role for bromine is further supported by the observation that the concentration of bromine is often higher in the contact regions of cuticular "tools", and, in this paper, a comparison of the mechanical properties of bromine-rich and unenriched arthropod cuticle also supports a functional role.

In order to measure a range of mechanical properties, we developed miniaturized versions of standard tests for wear and energy of fracture. We initially attempted to use an atomic force microscope (AFM) technique for measuring wear that has been used on similar specimens (Pontin et al., 2007) and involves repeated scanning of the measurement region in contact mode and recording the depth of the resulting pit. However, we found that this and similar AFM techniques failed one essential criterion for a wear test: repeated wear sessions did not continue to deepen the pit at the same rate. Thus our specimens appeared to have been indented rather than eroded. We also did not use AFM techniques for measuring energy of fracture because our AFM could not generate enough force to fracture some specimens, and because the AFM test is less direct. We did, however, use AFM techniques to measure modulus of elasticity, hardness and dynamic mechanical properties.

2. Experimental

2.1. Specimens

Specimens of *P. crassipes* (the lined shore crab) were collected on the coast of Oregon and California, and housed in an aquarium. The crabs were fed the alga *Ulva*, or, in a few cases, one or more of the following: crickets, pet rabbit food (The Hartz Mountain Corporation, Secaucus, NJ, USA), and marine invertebrate food (Tetra Tabi Min, Tetra Sales, Morris Plains, NJ, USA). When cheliped material was needed, a crab was caused to autotomize by lifting it quickly out of the aquarium by the desired claw. Specimens of the ants *Atta sexdens* and *Atta cephalotes* were selected from laboratory colonies to be full adults (as opposed to callows) as previously described (Schofield et al., 2002).

2.1.1. Maintaining hydration

In order to minimize any artifacts associated with changes in hydration, mechanical property measurements of *P. crassipes* and *Atta* were generally made within a couple of hours of extraction from the living organism and none were made more than 8 h after. During this period, autotomized claws were kept in sea water (similar to the laboratory environment and to the natural environment for a minor fraction of the day) until sample preparation. Ant samples were prepared immediately after dissection. After preparation, the samples were kept on an above-water platform in a closed container partially filled with water (near 100% RH at equilibrium). This environment was similar to the natural environment of the crabs during most of the day: *P. crassipes* is a high-intertidal organism and typically spends most of the day out of water but under wet rocks at our collection sites. Finally, cut surfaces of AFM specimens were sealed with epoxy to reduce loss of water, and abrasion test specimens were wetted during testing.

2.1.2. Other specimens

For comparisons of mechanical properties, we also collected *Pugettia producta*, the northern kelp crab, at Cape Arago in Oregon, and as representative non-calcified and calcified "tool" material in vertebrates, cat claw tips from a domestic cat and salmon teeth from a local fishmonger. These specimens were kept in a humid atmosphere and tested within one day of extraction from the living, or recently dead animal.

For X-ray absorption spectroscopy, the purple shore crab *Hemigrapsus nudus*, and polychaete worm *Nereis brandti* were collected near Coos Bay, Oregon, the sea spider *Ammothella tuberculata* was collected near Port Angeles, Washington, and the priapulid *Priapulus tuberculatospinosus* was collected in Germany. EXAFS spectra for air-dried and frozen hydrated spoon tips from *P. crassipes* were not distinguishable, so the mechanical parts of these other organisms were analyzed after air drying.

2.2. Abrasion resistance measurements

A custom "pin on disk" type abrasive-wear testing device was built for small (about 250 μm diameter) specimen pins (Fig. 2). The specimen pins were made using a 0.010″ (inside diameter) diamond core drill (Technodiamant, www.technodiamant.com). The cores were removed from the drill, oriented to wear the outside surface first, and affixed with cyanoacrylate gel adhesive to a steel pin held in the head of the wear tester (Fig. 3). This head was mounted on a custom-made load cell (measures force using a strain gauge [Vishay Micro-Measurements, Raleigh, NC]) that measured the horizontal force produced by friction between the specimen pin and the turntable (Fig. 2). During the wear test, the specimen pin was held against the turntable with adjustable weights that, for the standard test, produced a downward force of 0.019 N. The surface of the turntable was covered with wetted 600 grade abrasive paper (#413Q, 3M Corporation, www.3M.com), chosen instead of the more commonly used steel surface, in order to resemble the grain of rocks in the crab's environment. The turntable rotation period was 4 s, resulting in an interaction velocity of 0.027 m/s. After each 2 or 4 cycles of the turntable, the volume worn was calculated using a microscope to measure the diameter of the cylindrical pin and its change in length. The horizontal force was recorded continuously during the wear period; the average value of the force was used in later calculations. Several wear measurements were averaged to give a single value for each pin. The

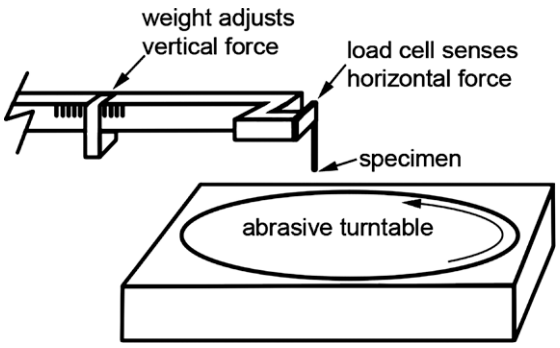

Fig. 2. Apparatus for testing abrasion resistance of small specimens. The arm holding the specimen pin is lowered to hold the specimen against the abrasive turntable with an adjustable force. The load cell measures the horizontal force as the rotating turntable abrades the specimen. The energy required to abrade the specimen is the product of the horizontal force and the distance traveled along the abrasive disk.

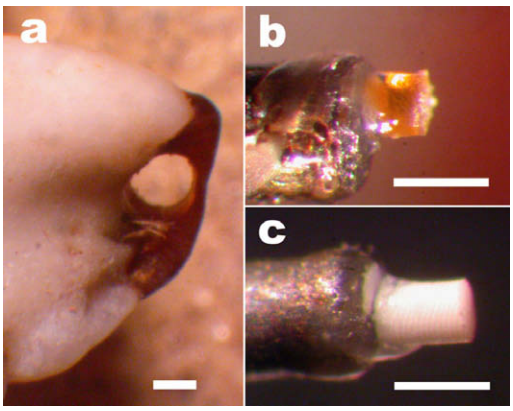

Fig. 3. Specimens for abrasion resistance testing. (a) A core drill has removed a circular plug from the bromine-rich region at the tip of the crab claw. (b) A core of translucent bromine-rich material bonded to the tip of a metal pin. The core has been abraded by the abrasive turntable of the testing apparatus. (c) A specimen of calcified cuticle. Scale bars: 500 μm.

wear rate (w), defined as the volume worn away per unit energy expended, was calculated as follows:

$$w = (\pi(D/2)^2 \Delta L)/Fd$$

where D is the diameter of the specimen pin, ΔL, the change in the length of the specimen pin due to wear, F is the force of friction measured by the load cell and d is the distance traveled by the pin over the abrasive paper.

2.3. Energy of Fracture measurements

A custom energy of fracture measuring device (employing the quasi-static work-area method for notched samples in tension) was built for 100 μm-scale fractures (Fig. 4). The specimens to be fractured were mounted between a load cell (Aerocon, www.aeroconsystems.com) and an optical translation stage (model 400, Newport Co., Fountain Valley, CA) that was driven away from the load cell by a powered micrometer (Oriel, Stratford, CT). The extension of the micrometer was measured to within 0.1 μm by counting pulses produced by the interruption of a light beam by shutters on the micrometer shaft. Both the force measured by the load cell and the extension of the micrometer were recorded by a computer to produce force–displacement curves. All parts of the apparatus were designed to minimize storage of energy within the apparatus as the specimen was stretched (Vincent, 1982). For example, energy storage in the load cell was minimized by using a stiff (low-displacement: the energy stored in the apparatus is proportional to the force and to the displacement of the apparatus) load cell (250 lb. limit) and amplifying the resulting small signal using a nanovolt DC amplifier (Keithley Instruments Model, 140, www.keithley.com). To test that most of the energy was being stored in the specimens, rather than the apparatus, a large piece of glass was mounted instead of a specimen. Because of its stiffness, very little energy was stored in the glass. The area under these control force–displacement curves demonstrated that the energy stored due to machine compliance was smaller than the energy stored within even our stiffest specimens. Collinear loading and unloading curves indicated that the energy stored in the machine and specimen was not depleted when the specimen was not fractured. We therefore assumed that the minor fraction of energy stored in the machine was used in fracturing the specimen, as long as the specimen fractured slowly, minimizing kinetic energy. The potential systematic bias in our results due to deviations from the assumption of static fracture would have been in the direction of increasing the energy of fracture value for calcified cuticle (thus minimizing the differences between cuticles) with an estimated maximum bias of no more than a few percent.

Fracture specimens were cut from the crab claws using either a razor blade (Personna super, American Safety Razor Company, www.asrco.com) or a 0.5-mm thick diamond saw blade (Dremel, www.dremel.com). The specimens were notched by hand, using a saw blade made from a razor blade with "teeth" made by drawing a second razor blade repeatedly across the cutting edge. The notched specimens were mounted (Fig. 5) between two microscope slide cover slips using a cyanoacrylate gel (Super Glue Gel, Elmer's Products, www.elmers.com) and/or a composite made from cyanoacrylate adhesive and 400-grit aluminum oxide powder, mixed to the consistency of clay. We found that it was essential to improve the bonding of the cyanoacrylate adhesives to the glass cover slips in the high humidity atmosphere by treating the cover slips with a 10-s dip in a 2% (by volume) 3-aminopropyltriethoxysilane (Sigma Chemical Co., www.sigmaaldrich.com), 98% acetone solution, followed by a rinse in deionized water and air drying. The two microscope cover slips bridged by the specimen were initially also bridged by a third cover slip, adhered with a temporary adhesive (ReMount, 3M Corporation, www.3M.com), that protected the specimen from accidental fracture by holding the cover slips at a fixed distance apart. The region of the notch in the specimen was then marked with a blue permanent marker, so that the fracture surface would be made evident by a lack of ink (Fig. 5). When the specimen/cover slip assembly was mounted in the fracture testing apparatus, the stabilizing cover slip was removed by dissolving the adhesive with ethanol. After the notched specimen had been drawn apart until fracture, the area of the fracture was measured using a microscope. This area was used to nor-

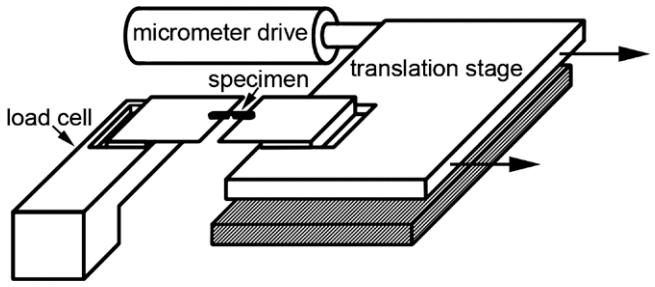

Fig. 4. Apparatus for testing energy of fracture of small specimens. The specimen bridges two microscope cover slips. One of the cover slips is attached to the load cell, the other to the translation stage. The translation stage is driven away from the load cell by the micrometer drive. The displacement of the micrometer and the force on the load cell are recorded by a computer to produce force–displacement curves. The area under one of these curves gives the energy required to produce the fracture.

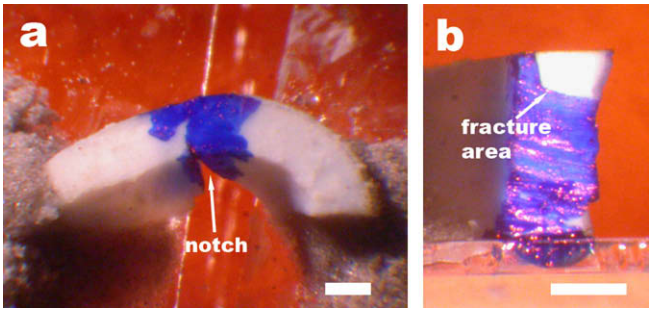

Fig. 5. Specimen of calcified cuticle before (a) and after (b) fracture. The curved piece of claw cuticle bridges two microscope cover slips which will be drawn apart in the plane of the figure. The fracture plane was perpendicular to the cuticle surface, which is the side with the larger radius. Scale bars: 500 μm.

malize force–displacement curves. The work of fracture per unit area of the fracture was obtained by numerically integrating these normalized force–displacement curves.

2.4. Hardness, modulus of elasticity and dynamic mechanical property measurements

Specimens were cut or ground until they appeared to be homogeneous (lacking structural features such as lumens and distinct changes in composition), and then mounted on atomic force microscopy (AFM) specimen disks (TedPella, Redding, CA) using an epoxy composite prepared by mixing about 0.4 g of 400-grit aluminum oxide powder with 0.075 mL each of 5-min-setting resin and hardener. The mounted specimens were placed in an oven at 39 °C for 20 min to cure the cement. This mounting technique was developed so that small "floating" silica specimens would yield the same hardness and modulus of elasticity values as large flat-mounted specimens (Schofield et al., 2002).

Hardness, modulus of elasticity and dynamic mechanical property measurements were made using an AFM (NanoScope IIIa, Digital Instruments, Santa Barbara, CA) with an add-on force/displacement transducer (TriboScope, Hysitron Inc., Minneapolis, MN). The Hysitron transducers hold a polished diamond probe in place with capacitors that are used to sense the position of the probe and to impart vertical forces for indenting and imaging the specimen.

We used an inverted pyramid-shaped diamond probe with cubic cornered facets (90° between the three faces) (Schofield et al., 2002). Except for discussed exceptions, the indentation sequence began with the force being ramped linearly from 0 to 2 millinewtons (mN) in either 0.01 or 1 s, maintained at 2 mN for 30 s and, when dynamic measurements were not desired, the force was ramped back to 0 over a period of 1 s. For dynamic measurements, after 30 s at 2 mN, the force was ramped down to 1.6 mN over 0.1 s and then the force was varied sinusoidally at 1 Hz (for 25 cycles) or 10 Hz (for 8 cycles) with a mean-to-peak amplitude of 0.2 mN. The force was then ramped to 0 in 1 s. These latter sequences allowed both dynamic and quasi-static properties to be measured.

A modulus of elasticity and a hardness value were obtained from force–displacement curves using the Oliver–Pharr technique (Oliver and Pharr, 1992, 2004). The Oliver–Pharr modulus of elasticity was obtained from the slope of the force–displacement curve at the beginning of withdrawal of the indenter. Oliver–Pharr hardness values were calculated from the intercept of this sloped line with the line of zero force.

In addition to the hardness obtained from the force–displacement curves, we also obtained a hardness value based on measurements of the size of the residual indentation. These residual indentation hardness values were calculated as $H = F/A$, where F is the maximum force applied to the probe, and A is the projected area of the residual indentation obtained from the perimeter of the indentation measured on an AFM image made by scanning the indenting probe itself immediately after indenting the specimen.

In the past we have not used the Oliver–Pharr technique and instead reported only these residual indentation hardness values (Schofield et al., 2002). This is because we found that the Oliver–Pharr method gave artificially low values when regions of the specimen buckled slightly because of voids such as poison ducts and lumens beneath the surface. The residual indentation hardness measurements, however, are not subject to this problem because they are not based on extension of the probe, only the force. For the present data, we do report results obtained with the Oliver–Pharr technique because the specimens were approximately homogeneous. Nevertheless, we did monitor the data for inconsistencies between the Oliver–Pharr hardness and the residual hardness, which could indicate a difference between the depth of the indent and the extension of the probe. The few cases that yielded different values were determined to be samples that had partially separated from the cement and were thus remounted or rejected.

Dynamic mechanical properties were measured from the sinusoidal segments of the indentation sequence by comparing the amplitude and phase of the displacement to the applied sinusoidal force (Lakes, 1998). Phase delays associated with the transducer and electronics were determined using a fused silica standard under an identical indentation sequence.

2.4.1. Calibration for Oliver–Pharr measurements

In order to obtain the contact area from the indent depth, the shape of the indenting tip must be known. We characterized the indenting tip shape directly using environmental scanning electron microscope images of the tip, instead of the usual method of back-calculating a tip shape that gives the expected values for a calibration specimen (usually fused silica), because we could not make indents in silica as deep as the indents in our softer specimens without fracturing the silica. The tip shape was characterized by three measurements: first the angle of the three-sided pyramidal tip (α), second, a measure of the distance between the apex of an ideal pyramid and the actual tip, the bluntness of the tip (B), and third, a measure of the distance from the blunted tip beyond which the shape of the tip was not distinguishable from an ideal pyramid (I). Only indents with greater depth than 'I' were used to calculate mechanical properties. The projected area (A) of the contact region between the tip and the specimen was calculated as:

$$A = (0.433)(4)(D + B)^2/((1/\tan^2(\alpha/2)) - 0.3333)$$

where D is the depth of the indent, determined by the extension of the indenting probe. As an example, the tip used for the majority of measurements was characterized by $\alpha = 89.9°$, $B = 122$ nm, $I = 86$ nm. Thus, for indents with a depth greater than 86 nm, $A = 2.58\ (D + 122\ \text{nm})^2$.

2.4.2. Measurement of residual indentation area

The area of the residual indent was measured using an SPM image, obtained immediately after the indent, using the indenting tip as the imaging tip. To minimize inaccuracies in indent perimeter determination caused by finite size of the imaging probe or other systematic errors, we only used indents with a depth of greater than 200 nm and we calibrated our area measurements so that we obtained a mean value of 70 GPa for measurements of the modulus of elasticity of fused silica.

2.4.3. Measurement of modulus of elasticity using the SPM image of residual indent area

We also used the area of the residual indent to calculate a modulus of elasticity value that does not rely on extension of the probe, and has been suggested for specimens that may be subject to "pile-up" artifacts (Oliver and Pharr, 2004).

2.5. Scanning electron microscopy

Air-dried specimens were Au–Pd sputter-coated and examined using a field emission scanning electron microscope (Amray 3300FE).

2.6. Transmission electron microscopy

Air-dried or frozen chela samples were rinsed in 70% ethanol, infiltrated with three changes of L.R. White resin, and polymerized for 24 h at 70 °C. Freshly obtained chela samples were fixed in 2.5% glutaraldehyde, 1.25% paraformaldehyde in 0.1 M cacodylate buffer (pH 7.3), dehydrated in an ethanol series and embedded in

L.R. White. Thin sections were collected on gold grids. Labeling with wheat germ agglutinin (WGA)-colloidal gold (15 nm) (EY Laboratories, www.eylabs.com) followed the method described in Steinbrecht and Stankiewicz (1999). Samples were examined with a Philips CM12 transmission electron microscope, operated at 80 kV.

2.7. High-energy ion microprobe elemental analysis

Data were obtained using two high-energy ion microscopy techniques: particle-induced X-ray emission, to measure the quantity of specific elements in the sampled volume, and scanning transmission ion microscopy, to measure the total quantity of material in the sampled volume (Schofield, 2001; Schofield and Lefevre, 1993). Combining the results of these two methods allows the determination of elemental concentrations within each sample volume.

2.8. Ion chromatography and amino acid analysis

Cheliped tips from each individual were analyzed separately. They were dissected, weighed, and hydrolyzed in 6 N HCl for 24 h at 110 °C in sealed glass ampoules. Hydrolysates were analyzed for bromine with a Dionex ICS 2000 ion chromatography system. Amino acid analysis of hydrolysates took place at the Molecular Structure Facility at the University of California, Davis (http://msf.ucdavis.edu), using ion-exchange chromatography to separate amino acids, followed by a "post-column" ninhydrin reaction detection system.

2.9. X-ray diffraction

Air-dried samples of cheliped spoon tips were examined at room temperature with Cu-α radiation using a Rigaku RU H3R X-ray diffractometer.

2.10. Scanning X-ray microscopy and microprobe spectroscopy

Scanning transmission and X-ray fluorescence microscopy and microprobe spectroscopy data were collected on beam line 9-3 at Stanford Synchrotron Radiation Lightsource (SSRL, SLAC National Accelerator Laboratory) using a modified version of the setup described by Pickering et al. (2003). The beam line was operated in a focused configuration with a pre-monochromator mirror performing vertical collimation and harmonic rejection (mirror cutoff at ~15 keV) and a post-monochromator mirror providing vertical and horizontal focusing. A glass monocapillary (X-ray Optical Systems, Inc., www.xos.com).) was used to further concentrate the beam to a size of ~10 × 10 μm (FWHM) at a working distance from the tip of 2 mm. Beam size was measured by differentiation of vertical and horizontal knife-edge scans. Samples were mounted on glass rods connected to magnetic mounts and were positioned and raster scanned in the X-ray beam using an XYZ stack of Newport PM500 stages topped with a rotation stage (Newport SR50CC). X-ray fluorescence for mapping and spectroscopy was measured using a single element silicon drift detector (Vortex EX-60, SII Nano Technology USA Inc.). Samples were raster scanned in point-to-point mode to collect images, then positioned to collect XAS data at points of interest. All measurements were performed at room temperature. Software for raster scanning and image visualization at the beam line were as described in Pickering et al. (2003).

2.11. X-ray absorption spectroscopy (XAS)

XAS data were collected on beam line 9-3 of SSRL. Harmonic rejection was achieved by the focusing mirror being configured to a nominal 15 keV cutoff. We used a 30-element intrinsic Ge solid-state detector and Z–1 fluorescence filter with Soller slits to record the XAS fluorescence signal from samples. The model compounds were measured using transmission mode. Bromine model compounds were purchased from Aldrich (www.sigmaaldrich.com) and included brominated aromatic compounds, bromo-L-phenylalanine and dibromo-L-tyrosine, as well as a brominated aliphatic model 2-bromohexadecanoic acid. XAS data reduction was carried out to extract EXAFS using the EXAFSPAK program. The theoretical phase and amplitude functions were calculated by FEFF 8.0.

XAS data of desired model compounds are not always available. To evaluate proposed structural models, we used calculated Debye–Waller factors (DWF) to simulate the EXAFS. To calculate these Debye–Waller factors, force constants for all bond–atom pairs were first calculated using the UFF force field (Rappe et al., 1992). We use the recursion method incorporated into FEFF 8.0 to calculate the DWF from the force constants. This method has been proven to be adequate to simulate the EXAFS of relevant models (Hsiao et al., 2006). With calculated DWF and amplitude and phase functions, we can simulate the EXAFS for comparison with measured data. Only E_0 was optimized by EXAFSPAK during these simulations.

3. Results and discussion

3.1. Ultrastructure and composition

Scanning electron microscope (SEM) images of the bromine-rich and calcified regions are shown in Fig. 6. The bromine-rich spoon tip was characterized by laminae, visible as thin sheets in Fig. 6, that are oriented perpendicular to the cuticle surface, and, imbedded in this matrix, large tubes (≈5 μm diameter), that ran from the interior of the claw to regions of the cuticle surface away from the sharp edges. The spacing of the laminae in transmission electron micrographs (not shown) was about 7 nm. The 5 μm tubes were hollow and breached the cuticle surface: we found that when the tip of a freshly autotomized claw was dipped in sea water containing colorants, the colorants were soon visible in the interior of the tubes. One possible function of these tubes is as conduits for chemoreception, like the funnel canals described in several crab species (Barber, 1961). The tubes and laminae are oriented perpendicular to the surface, and the expectation, confirmed below, is that fractures perpendicular to the surface, along the interfaces, would require less energy (e.g. wood fractures easily along grain interfaces).

The concentration of bromine in the spoon tips was found to be about 1% of dry mass, using multiple techniques, high-energy ion microprobe analysis, ion chromatography and plasma mass spectrometry. The microprobe analysis also revealed levels of calcium that were typical of levels in non-calcified insect cuticle (<1% vs about 30% in the calcified region). One of the spoon tip specimens was collected within one day of ecdysis, and it had a full complement of bromine. This limited sample suggests that bromine is incorporated into the crab cuticle at an earlier stage than zinc and chlorine in ant cuticle, and so highlights potential differences in the incorporation process for the different halogens (Schofield et al., 2003).

Along with bromine, the spoon tips contain protein and chitin. Amino acid analyses of hydrolyzed spoon tips indicate that the quantified amino acids (tryptophan, cysteine, and methionine were not quantified) account for 0.35 ± 0.1 of the mass ($n = 7$; all ± values in this paper indicate the standard deviation). X-ray diffraction of the spoon-tip yields a fiber pattern that corresponds to that of α-chitin microcrystals (Minke and Blackwell, 1978). Col-

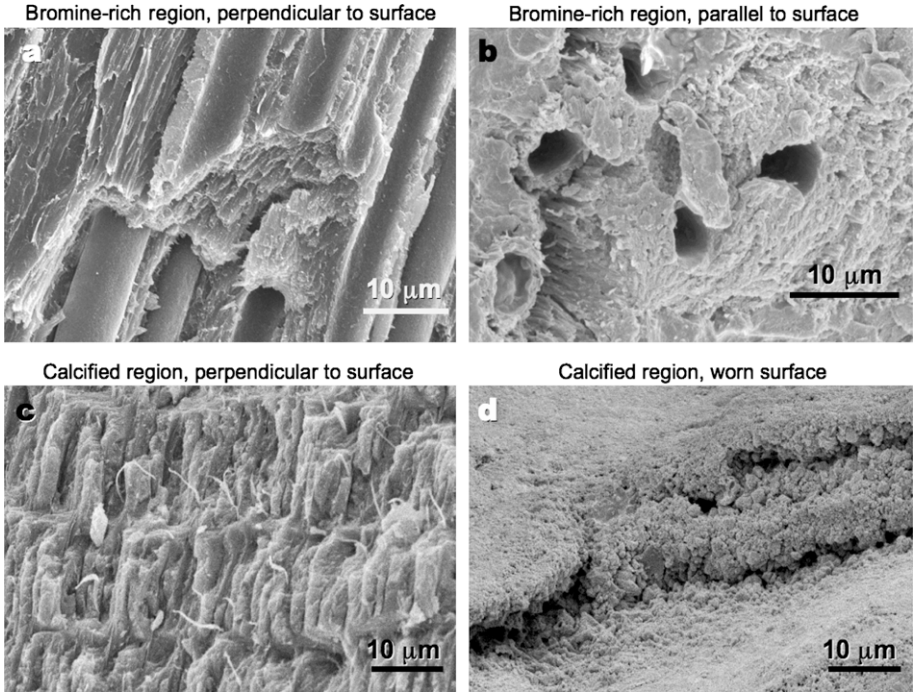

Fig. 6. SEM images of the bromine-rich (a and b) and calcified (c and d) regions of a cheliped of *Pachygrapsus crassipes*; image planes are perpendicular (a and c) or parallel (b and d) to the cuticle surface. Images a–c are of fractured surfaces, while d is of a naturally worn surface. Thin laminae and ~5 μm tubes run perpendicular to the cuticle surface in the bromine-rich region. In the calcified region (c), layers of ~2 × 15 μm calcite crystals are arranged with their long axis perpendicular to the cuticle surface. Fractures in planes perpendicular to the surface (a and c) could contain more interface between structures than parallel fractures (b and d), and thus are likely to require less energy (confirmed for the bromine region). The fibers visible in the calcified region (c) and tubes in the bromine-rich region (a) may increase the energy of fracture by requiring energy to pull out.

loidal gold-labeled wheat germ agglutinin (WGA), which binds specifically to N-acetyl glucosamine, was used to locate the chitin in the TEM. Gold label accumulated throughout the spoon-tip except for the walls of the 5 μm tubes, which may be composed entirely of proteins.

The calcified region contains chitin, proteins and calcite (Roer and Dillaman, 1993). Like the bromine-rich region, the calcified region is expected to be more difficult to fracture in a plane parallel to the surface because the perpendicular fracture could contain more crystal interfaces.

The non-calcified bromine-rich region appears to be homologous to the calcified region, rather than to the thin non-calcified layer that overlies the calcified region. There are two findings that support this contention: first, Fig. 7 shows that there are structures, part of the organic matrix framework, that appear to be continuous between the calcified and bromine-rich regions, and second, our WGA-labeling experiments indicated that the thin layer covering the calcified region does not contain chitin, while the bromine-rich region shows chitin labeling throughout, right to the exterior surface.

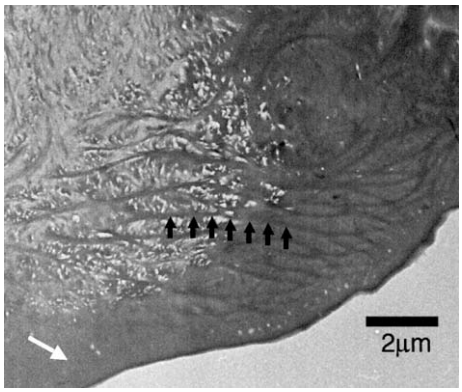

Fig. 7. Continuity of structure between the calcified and bromine-rich regions of the cheliped tip of a recently molted *Pachygrapsus crassipes*. The white regions in the mottled left side of the TEM image are empty spaces that would have been filled with calcite as the crab aged. Structural features (one is indicated by black arrows) in this region appear to continue into the region on the right hand side of the image, which is the base of the non-calcified bromine-rich region. This is evidence that the bromine-rich region is homologous to the calcified region and not to the ≈1 μm thick, chitin-free, non-calcified surface layer (white arrow) that covers the calcified cuticle and appears to extend a ways into the bromine region.

3.2. The local structural environment of bromine

X-ray absorption spectroscopy (XAS), was used to provide information on the type and spacing of the atoms surrounding the bromine atoms in the spoon tips and tarsal claws of the crabs. The results indicate that the average environment in the brominated cuticle is similar to the environment in bromophenyl-containing compounds.

Bromine EXAFS data for a dissected spoon tip display a major first-shell Fourier transform (FT) peak arising from a Br–C interaction at a distance of 1.87 Å (Fig. 8c, bold solid line). This Br–C distance is similar to that found in bromoaromatic compounds, so we compared these data with bromine EXAFS of two model compounds, bromo-L-phenylalanine (Fig. 8b1 and c1, bold dotted line) and dibromo-L-tyrosine (Fig. 8b1 and c1, bold dashed line). Both of these compounds display first-shell FT peaks that are very similar to that from the spoon tips, as well as 2.9-Å FT peaks from the β carbons in the phenyl ring (note that the 5.7-Å FT peak in the data for dibromo-L-tyrosine likely results from Br–Br scattering). In contrast, bromine EXAFS for the bromoaliphatic model compound, 2-bromohexadecanoic acid (Fig. 8c2, thin solid line), displays a first-shell FT peak at a significantly longer Br–C distance. The bro-

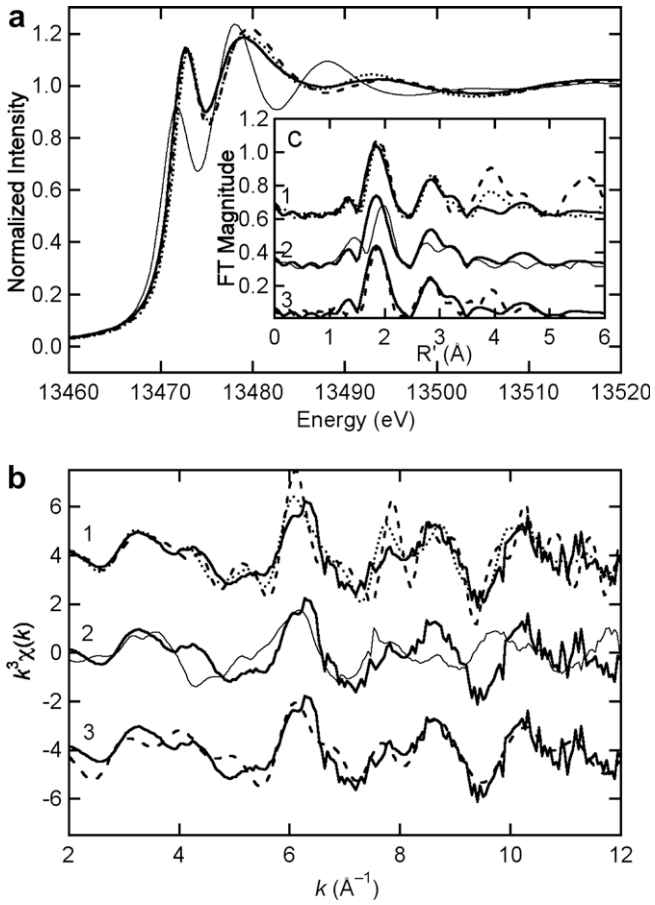

Fig. 8. The bromine K edge X-ray absorption spectra of a frozen hydrated *Pachygrapsus crassipes* crab claw spoon tip (sample #5) compared with standards and simulated data. Plot a is of the bromine edge region, b is the EXAFS, and insert c is the Fourier transform (k = 2–12 Å^{-1}; k^3 weighted). All bold solid lines are for a crab claw spoon tip. The spoon tip tissue data are compared with bromophenyl chemical standards in a, b1, and c1 (bold dashed: 2,4-dibromo-L-tyrosine, bold dotted: 4-bromo-L-phenylalanine); a bromoalkyl chemical standard in a, b2, and c2 (thin solid: 2-bromohexadecanoic acid); and simulated data for bromobenzene in b3 and c3 (bold dashed line). Bromine XAS data for the crab claw spoon tip is consistent only with a single bromine atom bonded to a phenyl ring.

mine edge (Fig. 8a) and EXAFS (Fig. 8b2) are also distinct from the data for the spoon tip. We also used the modeling code FEFF to simulate the expected bromine EXAFS for a simple bromobenzene model (Br–C = 1.87 Å, C–C = 1.42 Å) and this simulation is displayed in Fig. 8b3 and c3. This simulation reproduces the main features in both the EXAFS and the FT. A simulation based on a bromohistidine model gave a first-shell Br–C distance that was more similar to that of the brominated cuticle, but did not reproduce outer-shell FT peaks as well as bromobenzene (data not shown). In summary, the bulk bromine EXAFS data are consistent with binding of the crab cuticle bromine to an aromatic ring, most likely provided by an amino acid.

As a feasibility test, we checked that there are enough binding sites to bind the percent levels of bromine. Amino acid analysis of several specimens indicated that there was about one atom of bromine for every two tyrosine residues. This may be an overestimate if the tyrosine estimate is low because of cross-links that resist acid hydrolysis. In either case, there appears to be plenty of tyrosine binding sites.

An additional suggestion that bromine was bound by tyrosine was that the fraction of tyrosine in amino acid analyses was about 10 times greater in the bromine-rich spoon tip than in adjacent calcified regions of the claw; this order of magnitude difference did not apply to phenylalanine content (bromine-rich region: 4.8 ± 0.8% tyrosine, 2.4 ± 0.4% phenylalanine (eight specimens); calcified region: 0.4 ± 0.3% tyrosine, 1.7 ± 0.7% phenylalanine (three specimens)).

Bulk bromine XAS provides structural information averaged across the entire specimen. To investigate the homogeneity of the bromine structural environment, we used scanning X-ray microscopy and microprobe X-ray spectroscopy at a spatial resolution of about 10 μm. Fig. 9 shows that the bromine is smoothly distributed throughout the spoon tip (note that the variation in Br content shown in Fig. 9 has not been corrected for sample thickness; the lower Br content near the edges may simply be a result of reduced sample thickness). We then set the specimen so that several spatially separated spots were illuminated by X-rays while we collected bromine XAS data by fluorescence excitation. Fig. 9 shows that the bromine edges obtained at these locations are all virtually identical and are also very similar to the edge recorded in the bulk bromine EXAFS experiment (Fig. 8a). From this admittedly limited sampling, it appears that the bromine speciation is homogeneous across the spoon tip and that the bulk bromine EXAFS is representative.

Similar XAS results to those from the spoon tips were obtained for a variety of structures and organisms (Fig. 10): the tarsal (leg) claw of another grapsid crab, *H. nudus*; the tarsal claw of a chelicerate, the sea spider *A. tuberculata*; the jaw tip of a polychaete worm, *N. brandti*; and pharyngeal teeth of the priapulid, *P. tuberculatospinosus*. The profile, intensity and position of edges are almost identical. The EXAFS also exhibits similar main features, such as the splitting at ~4 and ~8 Å^{-1} and the shoulder at ~5 Å^{-1}. The Fourier

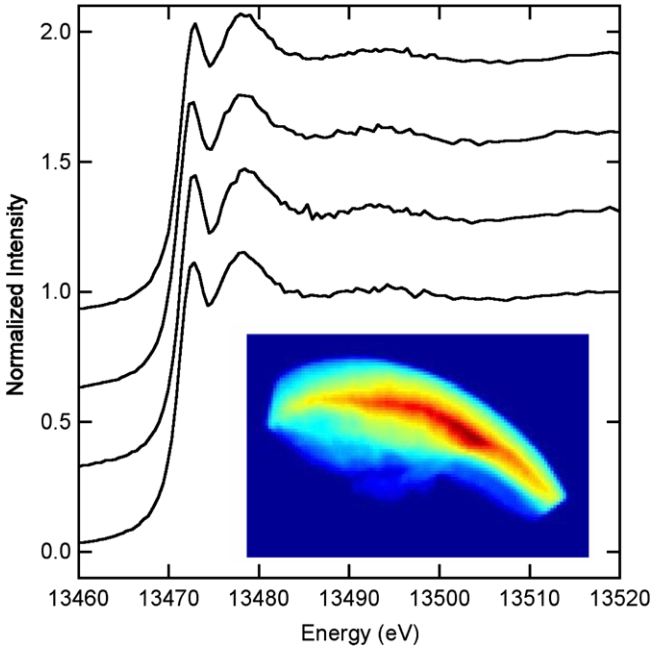

Fig. 9. The inset is an image of the bromine K_α fluorescence emission intensity [in arbitrary units ranging from zero (dark blue) to highest (dark red)] recorded on a crab claw tip specimen by scanning fluorescence X-ray microscopy with excitation at 14 keV. The X-ray beam size was ≈10 × 10 μm and the raster step size was 10 μm. The horizontal dimension of this image is 2.0 mm. The upper convex edge of the bromine emission coincides with the external surface of the crab claw tip while the bottom represents the dissection region. Four spots across the bromine content of this specimen were selected to collect bromine XAS edge spectra and these spectra (single first sweeps) are displayed above the inset image. The shape and structure of these edges are sensitive to the local bromine environment (cf. a) and all appear identical to one another and very similar to the edge observed in the bulk bromine XAS experiment, suggesting a homogeneous bromine environment well represented by the EXAFS data in Fig. 8.

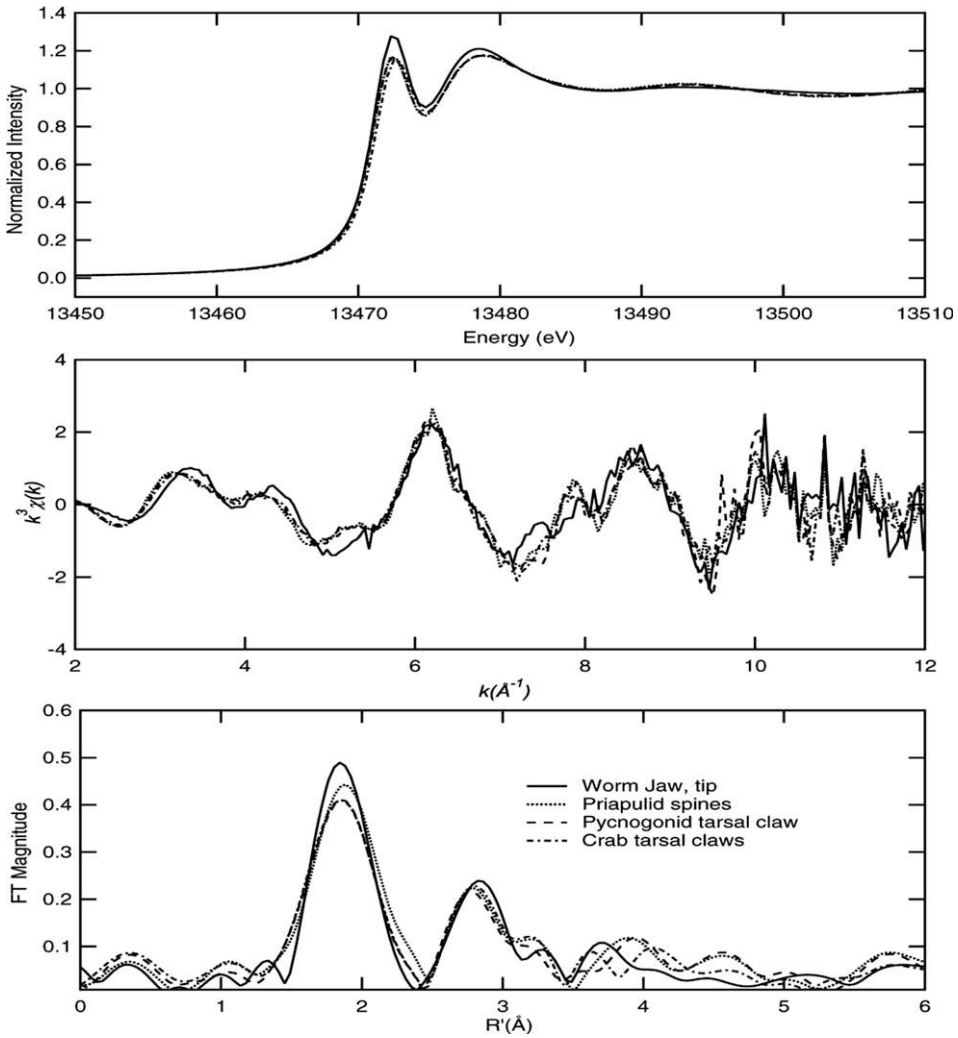

Fig. 10. Bromine XAS data are similar for distantly related organisms. Fourier transforms used EXAFS data from $k = 2.0–12.0$ Å^{-1}, k^3 weighting, with phase shift correction, based on Br–C scattering. Solid lines: jaw tip from the worm *Nereis brandti*; dotted line: pharyngeal teeth from the priapulid *Priapulus tuberculatospinosus*; long dashed line: tarsal (leg) claw of the pycnogonid *Ammothella tuberculata*; short dashed line: tarsal claw of the crab *Hemigrapsus nudus* (from Tao et al., 2007).

transform also shows similar peaks. This suggests similar bromine coordination environments in all of these organisms, reminiscent of monobromoaromatic species.

3.3. Mechanical properties I: abrasion resistance, coefficient of kinetic friction, energy of fracture, hardness and modulus of elasticity

3.3.1. Calcified cuticle is slightly more abrasion resistant than bromine-rich cuticle

Table 1 shows that the calcified cuticle was about 30% more abrasion resistant than bromine-rich cuticle ($p = 0.038$, Wilcoxon two-sample test (Lupton, 1993)).

To test sensitivity to the vertical force, four specimens were re-run using a 10 times greater force to press them against the abrasive paper. The results were statistically indistinguishable from the values for the nominal 0.019 N used in Table 1.

3.3.2. Coefficients of kinetic friction are similar for brominated and calcified cuticle

The values of the coefficient of kinetic friction, the ratio of the force of friction measured in the wear test to the force pressing down on the specimen, were not quite statistically distinguishable for calcified and brominated cuticle (calcified: 0.71 ± 0.06; bromine-rich: 0.64 ± 0.03; seven specimens in each case; $p = 0.057$, Wilcoxon two-sample test).

3.3.3. Energy of fracture is 9 times greater for bromine-rich than for calcified cuticle

The energy of fracture columns of Table 1 show that nearly an order of magnitude more energy was required to produce a fracture of a particular area in Br-rich than in Ca-rich cuticle. Fig. 11 shows the data for specimens that yielded median values. The potential area of a fracture depends both on the energy of fracture and on the energy available for fracture, and will be discussed below along with environmental challenges.

We tested the hypothesis that the energy of fracture depends on the orientation of the fracture planes (see Fig. 6). Fractures that are transverse to the tips (diagram in Fig. 12) could sever the tips, and so are probably the more dangerous type. Table 1 shows that transverse fractures of the spoon tips required about 1.5 times the energy to produce than fractures that were perpendicular to the surface (Wilcoxon two-sample test: $p = 0.008$). For calcified claw teeth, the fracture resistance values were also higher for the transverse plane, but because the measurement variation was greater, the difference was not significant ($p = 0.09$).

Table 1
Quasi-static mechanical properties.

Material	Wear rate (w), mm^3/J	n	Energy of fracture (K), J/m^2				Hardness (H), GPa		Reduced modulus of elasticity (E), GPa		n	Force challenge[e] $\sqrt{(KE)}$	Displacement challenge[e] $\sqrt{(K/E)}$
			Transverse to cuticle projection[d]	n	Perpendicular to cuticle surface[d]	n	Oliver–Pharr	From image[c]	Oliver–Pharr	From image[c]			
Calcified crab cuticle (*P. crassipes*)	0.8 ± 0.2 M = 330	7	348 ± 138 M = 210	6	233 ± 65	7	1.49 ± 0.40	1.79 ± 0.35	35 ± 12	35 ± 11	38	3.4×10^6	1×10^{-4}
Bromine-rich crab cuticle (*P. crassipes*)	1.0 ± 0.2 M = 2930	7	2931 ± 574 M = 2005	8	1991 ± 551	6	0.49 ± 0.12	0.60 ± 0.08	7.6 ± 2.7	7.6 ± 2.2	45	4.7×10^6	6.2×10^{-4}
Un-enriched ant cuticle (*Atta sp.*)			3885 ± 2514 M = 3423	9	1557 ± 545 M = 1690	8	0.33 ± 0.07	0.37 ± 0.06	5.2 ± 1.6	5.0 ± 1.6	35	4.1×10^6	8.3×10^{-4}
Cat claw (keratin)			13321 ± 8810 M = 12684	9			0.31 ± 0.03	0.35 ± 0.02	5.5 ± 0.5	5.3 ± 0.3	6	8.2×10^6	15×10^{-4}
Salmon tooth			2255 ± 649 M = 2088	5			1.13 ± 0.01	1.30 ± 0.04	23 ± 1.2	23 ± 1.4	3	6.9×10^6	3.0×10^{-4}
Calcified crab spoon tip cuticle (*Pugettia producta*)							1.4 ± 0.1	1.5 ± 0.2	32 ± 3	30 ± 2	3		
Nylon 6 (not dried)	0.30	1					0.20 ± 0.01	0.14 ± 0.01	3.1 ± 0.14	2.5 ±0.16	3		
PMMA (acrylic)							0.33 ± 0.04	0.29 ± 0.07	6.8 ± 0.8	5.9 ± 0.6	14		
Polycarbonate							0.26 ± 0.004	0.25 ± 0.004	3.2 ± 0.04	2.8 ± 0.03	3		
Fused silica							10.7 ± 0.7	12.8 ± 1.7	71 ± 8	[a]70 ± 12	[b]		

M: median, which is less sensitive to out-lying samples that may not have fractured quasi-statically.
n: number of specimens.
[a] This value was set to 70 GPa by adjusting the calibration factor for the area of the indents. This calibration factor is used to account for systematic errors in measuring the area of the indentation using SPM images. This area calibration factor was used in calculating all other image-based hardness and modulus of elasticity values. The Oliver–Pharr measurements were not adjusted to give a particular value, instead, they are derived from ESEM measurements of the indenting tip shape and the factory calibration of the force and displacement of the indenting transducer. The fact that the resulting value, 71 GPa, for fused silica is close to the accepted value of 70 GPa, is evidence that the factory instrument calibration is correct.
[b] n = 14 for values from images and n = 28 for Oliver–Pharr values.
[c] Areas measured on AFM images of the residual indentations were used in the calculation.
[d] For fracture orientations, see Fig. 11.
[e] For "K", the transverse median value was used, for "E", the image value was used.

3.3.4. Bromine-rich cuticle is intermediate in hardness and modulus of elasticity between calcified cuticle and bromine-free ant cuticle

Table 1 also shows that calcified cuticle is roughly 3 times as hard and has a 5 times greater modulus of elasticity than bromine-rich cuticle. For a comparison between the bromine-rich crab cuticle and non-enriched arthropod cuticle (all examined cuticle from the crabs was either calcified or brominated), bromine-free cuticle from the mandible of leaf-cutter ants is included in the table (the tested material was not from the Zn-rich mandibular teeth). While bromine-rich spoon tip cuticle is not as hard as calcified cuticle, it is 1.6 times as hard and has a 1.5 times greater modulus of elasticity than the bromine-free cuticle from the ant mandibles. This difference further supports a functional role for bromine in arthropod cuticle.

For viscoelastic and plastic materials, the measured values of modulus of elasticity and hardness can vary with the duration of the applied force. We compared our standard quasi-static indent regime (1 s ramped increase in force, 30 s constant force, 1 s withdrawal) to a shorter regime (0.1 s ramp, 0.5 s constant force, 0.1 s withdrawal) on some specimens. We found no significant difference for calcified cuticle, but for brominated cuticle, the measured modulus of elasticity and Oliver–Pharr hardness for the shorter regime increased by a factor of 1.4, and residual indent hardness increased by 1.2. Thus the differences in hardness and modulus of elasticity between calcified and brominated cuticle should be less for interaction times that are shorter than the 32 s used for Table 1. This effect points to the importance of measuring the dynamic as well as the quasi-static mechanical properties.

3.4. Mechanical properties II: dynamic mechanical properties

Dynamic properties at two frequencies are tabulated in Table 2. The energy stored during the sinusoidal indentation is proportional to the storage modulus, while the energy lost as heat is proportional to the loss modulus. The ratio of loss modulus to storage modulus is the loss tangent ($\tan(\delta)$). Greater values of loss tangent indicate greater damping of vibrations and greater attenuation of propagated waves (Ferry, 1980; Lakes, 1998, Vogel, 2003). The loss tangent is, at 10 Hz, roughly 5 times greater for brominated than for calcified cuticle, indicating that a 5 times greater fraction of stored energy is lost, and not available for fracture, each cycle.

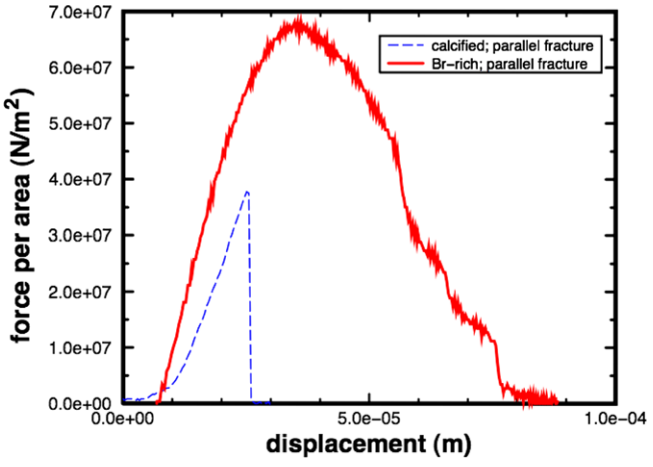

Fig. 11. The work required to produce a fracture is much greater for bromine-rich claw cuticle than for calcified claw cuticle. The curves for these two specimens were selected for display because they yielded median values of energy of fracture for fracture planes mostly parallel to the cuticle surface (since n was even in each case, two median values were averaged to give the median value in Table 1). To produce this plot, force–displacement curves from the testing apparatus were normalized by the measured area of the fracture. The area under these curves is the work per unit area required to produce the fracture; for the bromine-rich cuticle specimen, 2800 J/m^2, for the calcified cuticle specimen, 330 J/m^2. These are scaled raw curves: curves that had been corrected for machine compliance yielded insignificantly different values, as expected. The multiple steep drops on the right hand side of the bromine-rich curve indicate a gradual release of stored energy (Vincent, 1982), suggesting that most of the energy went into forming the fracture. This is not clear from the single sharp drop for the calcified specimen, but other calcified specimens with values near the median did have multiple drops.

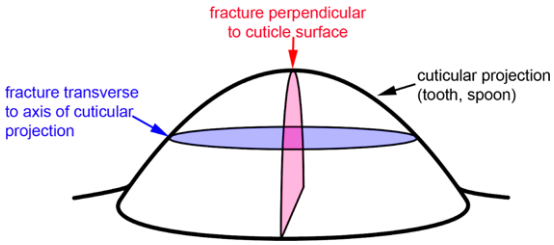

Fig. 12. Diagram showing the two different planes of fracture. The transverse fracture plane is roughly parallel to the cuticle surface at its center.

The highest frequency we could achieve using our apparatus was 10 Hz, which may be representative of the peak frequencies associated with low force clamping or scraping, but is very low compared to peak frequencies associated with impacts, such as when the claw slips, accelerates because of continued force, and impacts the environment. For impacts that occur at, for example, a moderate velocity of 1 m/s, and produce a depression of 1 μm, the dominant period in the Fourier decomposition of the surface displacement would be roughly 4 times the time from zero to maximum indentation (Main, 1978), or, with a uniform deceleration and no other movement of the claw, a frequency of about 2.5×10^5 Hz. While we have not measured dynamic mechanical properties and damping for these relevant high frequencies, we have qualitatively compared the resistance of calcified and bromine-rich cuticle to such impacts. Fig. 1b shows that calcified cuticle erodes more rapidly than bromine-rich cuticle when subjected to the multiple impacts of small high-velocity glass beads.

3.5. Advantages of calcified, bromine-rich, and unenriched cuticle for different environmental challenges

3.5.1. Force challenge and the effects of non-local energy storage

Susceptibility to fracture depends on the energy required per unit area of fracture, and on the energy available for fracture. The stored energy is an upper limit to the energy available for fracture and is equal to the force multiplied by the incremental distance that the material (analogous to a spring) compresses. Thus, for a given force and shape, less energy is stored in a material that has a high modulus of elasticity and so compresses less. As a result, the fracture resistance increases as the square root of the product of the energy of fracture and the modulus of elasticity (Ashby et al., 1995). This figure of merit is shown in Table 1. Brominated cuticle requires a 1.4 times greater force to produce a given fracture area than calcified cuticle (the difference is significant: $p < 0.05$). This difference is small because the greater energy of fracture of the brominated cuticle is partly compensated by its greater compression and energy storage. Nevertheless, our data suggest that brominated cuticle could resist a 1.4 times greater force than the actual calcified cuticle could for the same thickness of exoskeleton. If there is any advantage to calcified cuticle for an exoskeleton, it may be that the stiffness due to the higher modulus of elasticity allows for larger organisms and for less pressure on internal organs during an attack.

The above analysis assumes that the energy available for fracture is stored in the material being challenged, but if the construction is not homogeneous, energy can be stored non-locally in a

Table 2
Dynamic mechanical properties.

Specimen	Storage modulus (GPa)		Loss modulus (GPa)		tan(δ) (relative to silica)		Number of specimens
	1 Hz	10 Hz	1 Hz	10 Hz	1 Hz	10 Hz	
Calcified crab (*P. crassipes*) cuticle	36 ± 10	42 ± 10	2.1 ± 1.3	0.79 ± 0.65	0.06 ± 0.02	0.02 ± 0.02	20
Bromine-rich crab (*P. crassipes*) cuticle	7 ± 3	8 ± 2	0.8 ± 0.3	1 ± 0.3	0.12 ± 0.06	0.13 ± 0.07	21 (1 Hz) 19 (10 Hz)
Plexiglass (acrylic)	5.9 ± 0.03	6.7 ± 0.2	0.531 ± 0.006	0.73 ± 0.07	0.090 ± 0.001	0.108 ± 0.008	3
Nylon 6 (not dried)	3.16 ± 0.06	3.6 ± 0.2	0.27 ± 0.01	0.37 ± 0.02	0.086 ± 0.002	0.10 ± 0.01	3
polycarbonate	3.58 ± 0.06	3.86 ± 0.02	0.09 ± 0.02	0.23 ± 0.01	0.026 ± 0.004	0.060 ± 0.003	3
PMMA	6.6 ± 0.8		0.75 ± 0.27		0.11 ± 0.04		17

p for Wilcoxon two-sample test for tan(δ): 1 Hz Ca vs Br: $p = 1.3 \times 10^{-4}$; 10 Hz Ca vs Br: $p = 1.8 \times 10^{-7}$.

different material. If most of the displacement (and energy storage) resulting from the applied force is due to stretching of tendons or slight bending of large structures such as legs, then most of the energy storage is not in the spoon tips, and roughly the same amount of energy would be available whether the spoon tips were brominated or calcified. In this case the brominated cuticle could resist a roughly 3 times greater force than the calcified material could, for the same potential area of fracture, because the energy of fracture is greater by nine (this and other examples discussed here are simplified and assume that other factors, such as density of crack initiation sites, are equal).

Thus the fracture resistance of the tip is increased by the use of calcified material elsewhere, illustrating that there can be advantages to using stiff materials everywhere except at the contact surfaces.

3.5.2. Deformation challenge

In a deformation challenge, the material is subjected to a specific deformation rather than a specific force. If an algae-scraping spoon tip encounters a grain of rock small enough that it does not stop the spoon, a small region may be forced to deform around the grain or fracture. The material with the lowest modulus of elasticity (the softest spring) will store the least energy during the deformation. Thus the material that will allow the largest deflection before a fracture occurs, is the material with the highest value of the ratio of the energy of fracture to the modulus of elasticity ($\sqrt{(K/E)}$) (Ashby et al., 1995). The sixfold difference (Table 1) between calcified and bromine-rich cuticle suggests that the brominated cuticle can withstand a 6 times greater deformation than calcified cuticle.

This sixfold advantage is even further improved by the brominated cuticle's greater viscoelasticity. If the forced deflection takes place slowly, the energy stored in the brominated cuticle is partly used to rearrange the molecules and may not be released quickly enough to be available for fracture (the deformed structure springs back slowly). The slower the crab scrapes algae, the more the tip could deflect before fracture. There may be an optimal balance, between higher rates of food collection and greater risks of fracture, that varies according to the relief of the substrate.

The greater ability of bromine-rich cuticle to deform without fracture may also allow a more thorough, squeegee-like scraping of algae from rocks.

3.5.3. Abrasion challenge

Calcified cuticle is slightly (30%) more resistant than bromine-rich cuticle to the type of abrasion tested here. In the field, we have observed several individuals with severe abrasive wear (even penetrating the cuticle) on calcified regions of the claws that contacted the rock as the crab wedged in for shelter. Our data suggest that there would be no advantage to using brominated cuticle instead of calcified cuticle in these contact regions.

The roughly equal resistance to abrasive wear, even though the energy of fracture differs by an order of magnitude, may be associated with the size of the calcite crystals. If we hypothesize that the energy required to abrade away a volume of the cuticle is mainly used in creating the new surfaces of the abraded particles, then the expected particle diameter would be 1.6 μm for calcified cuticle and 18 μm for brominated cuticle. A cursory examination of the abraded particles produced in our test suggested that the particle diameter was of this order of magnitude. The factor of 9 greater surface area expected for eroded particles of calcified cuticle is apparently accounted for with more particles of smaller diameter. But this surface area condition could also be met if calcified cuticle instead eroded into fewer, larger particles than the particles of brominated cuticle, resulting in a greater wear rate for the calcified cuticle. The solution resulting in more smaller particles (and a roughly equal wear rate) may be favored because there is a natural particle size: Fig. 6 shows that the diameter of the calcite crystals (about 2 μm) is about the same as the particle diameter calculated from the wear rate for the calcified cuticle.

While the wear rate is about equal for these abrasive forces, as the force and stored energy increases, the potential size of fracture will increase until a whole tooth or structure can be severed; to reach this point, the stored energy would have to be 9 times greater for brominated than for calcified cuticle.

The expected advantage of brominated cuticle for these more energetic abrasions is probably further increased by its viscoelasticity. With a loss tangent of 0.13, the resonant vibrations of structures would be expected to be damped to $1/e$ of their original amplitude (and $1/e^2$ of energy storage) in only 2.5 cycles (Ferry, 1980; Lakes, 1998). This is likely to be particularly important when the energy input lasts longer than the period of a single cycle, such as during abrasive scrapes.

3.5.4. Pressure and indent challenges

If the spoon tips were made of calcified instead of brominated cuticle, they could apply greater pressures when used as forceps, because the higher modulus of elasticity would result in less deformation (~1/5 as much deformation as bromine-rich material for simple conditions).

In addition to being capable of applying greater pressures, the calcified material is also ~3 times as hard as the bromine-rich cuticle and so indentations produced by hard grains would be ~1/3 as large, in area, for the calcified material. Accumulations of these small damage features could ruin the forceps-like mating of opposing spoon tips.

In turn, the brominated cuticle would be better than unenriched cuticle for applying pressure because it is harder and has a higher modulus of elasticity. The apparent advantage of brominated over calcified cuticle is that it achieves a higher hardness and modulus of elasticity than unenriched cuticle without being significantly more prone to fracture.

3.5.5. Impact challenge

If a claw slips and impacts a rock, the energy of motion can be temporarily stored in the claw material near the impact site. This is analogous to the bead blasting experiment shown in Fig. 1: when the bead comes to rest before bouncing back, most of the energy of motion is stored in the claw because the glass bead has a higher modulus of elasticity. The potential fracture area from this stored energy would be 9 times greater for calcified cuticle than for brominated cuticle, consistent with the more rapid erosion of the calcified cuticle.

3.6. Fracture resistant materials in regions of low cross-sectional area

Fracture resistance is especially important in regions with small cross-sections where less energy is required to sever a structure. For example, to chip off the thin rim of the spoon tips (and ruin the forceps-like mating) or the tip of the sharp tarsal claw (and reduce the crab's ability to cling), would require a fracture with only a small surface area. On the main body of the crab claw or leg, a fracture of similar area would tend to cause little damage.

The susceptibility of regions with small cross-section to catastrophic fracture may be exacerbated by the tendency for energy to be stored (and available for fracture) in these same regions. A sideways force on a stiff leg or tarsus will tend to bend the leg most at the thin sharp tip. The stored energy density will be greatest in the region that bends the most, analogous to a compound spring where energy storage is greatest in the most compressible part of the spring. Thus the stored energy density will likely be greatest at the leg or spoon tip where it is readily available for a damaging fracture, and the bending may increase the likelihood of crack initiation.

As a result, there may be an adaptive advantage for the organism to trade desirable mechanical characteristics, such as hardness and high modulus of elasticity for resistance to fracture in these regions of low cross-section.

3.7. Patterns of damage

Fig. 13 shows that the patterns of damage to claws are consistent with our measured mechanical properties. The imaged crab claw had fracture damage to the calcified teeth but none was apparent on the thin rim of the spoon tip. Abrasive wear was evident in both calcified and bromine-rich cuticle.

3.8. Comparison with other biological and engineering materials

For comparison, Table 1 also includes other biological and engineering materials, tested using the same methods as the crab cuticle. While most of the values from these microscopic tests are comparable to values from macroscopic tests, the AFM test of the modulus of elasticity of the polymer PMMA yielded values of 6 or 7 GPa, while values from macroscopic tests are typically around 3 GPa (Giddings et al., 2001; Ishiyama and Higo, 2002). A possible explanation for this difference is that the size of the indentations for the AFM test are close to the size of the polymer molecules. Comparisons of microscopic measurements on biological materials to macroscopic measurements on engineering materials appear to have led to overestimations of the advantages of biological materials (Broomell et al., 2006).

If the tip of the crab claw were made of Nylon 6, it would be more resistant to wear but not as hard or as stiff as the bromine-rich cuticle. Even the hardest of the tested plastics, polymethyl methacrylate (acrylic glass), was only as hard as unenriched cuticle.

Cat claw samples were more resistant to fracture than the bromine-rich material, but, like the plastics, did not have as high modulus of elasticity or hardness. Salmon tooth samples were harder and had a higher modulus of elasticity, but could resist only about 1/2 the deflection that brominated cuticle could (the hardness and modulus of elasticity tests sampled the cap enameloid, while the fracture test sampled the whole tooth).

We also tested the spoon tips of the kelp crab *P. producta*, because they appear to be calcified instead of brominated, even though brominated cuticle is present in the tarsal claws. As expected, the hardness and modulus of elasticity were similar to that of the calcified regions of the claws of *P. crassipes*. A possible explanation for the absence of brominated cuticle in the spoons is that the kelp crab was collected and typically lives and feeds on large algae (Ricketts et al., 1985), where its claws are less likely to encounter hard rocks or grit. Furthermore, the spoons do not fit together like forceps. As a result, small fractures may be both less likely and less detrimental, making fracture resistance less important.

3.9. Fracture resistance in small organisms

The argument, detailed above, that fracture resistance is especially important in regions with low cross-sectional area leads to a hypothesis that smaller organisms are more likely to trade desirable mechanical properties, like hardness, for greater fracture resistance. For example, if the smaller organism is subjected to the same forces or impacts as a larger organism (such as from a particular predator, adversary, or environmental effect), then fracture resistance may be relatively more important because of the smaller cross-sectional areas of its mechanical structures.

In addition, smaller organisms produce smaller forces and, so, in order to produce pressures (force per area) that are equal to maximum pressures produced by larger organisms (e.g. to puncture or grasp a mutual food item such as algae), they must have smaller contact areas for their claw tips, teeth, stings, etc. The sharper structures (edges or points) are more susceptible to fracture damage.

A similar argument is that the presence of a fracture of a certain cross-sectional area may be more detrimental to a smaller organism because it may not be able to generate the greater force required to puncture or grasp with the blunted structure.

These arguments suggest that softer bromine-rich cuticle would tend to be employed more often by taxa of crabs that tend to be smaller, and, in general, that materials with the balance of mechanical properties weighted towards fracture resistance, will tend to be employed more often by smaller organisms.

In addition, smaller organisms might also minimize the chance of catastrophic fracture of their tools by behavioral adaptation. For example, they might tend to apply forces more slowly, when possible, to take advantage of viscoelasticity and to minimize uncontrolled forces that can lead to fracture.

3.10. Chemistry and mechanical properties

The mechanism by which brominated phenyl rings modify the mechanical properties of the cuticle is not understood. Pryor (1962) suggested that electrophilic halogens would generate a partial positive charge on the phenolic hydroxyl groups, which might then participate in cross-linking reactions. An increased density of cross-links would likely increase the modulus of elasticity and the hardness, consistent with the differences between unenriched and bromine-rich cuticle. An additional possibility is that the mass density of the heavy atom plays a mechanical role. This hypothesis would help explain why many structural materials in invertebrates are modified with heavy atoms, Mn, Fe, Cu, Zn, Br, and I (Schofield, 2001). Damping of mechanical vibrations in polymers has been associated with molecular motions that occur at the same frequen-

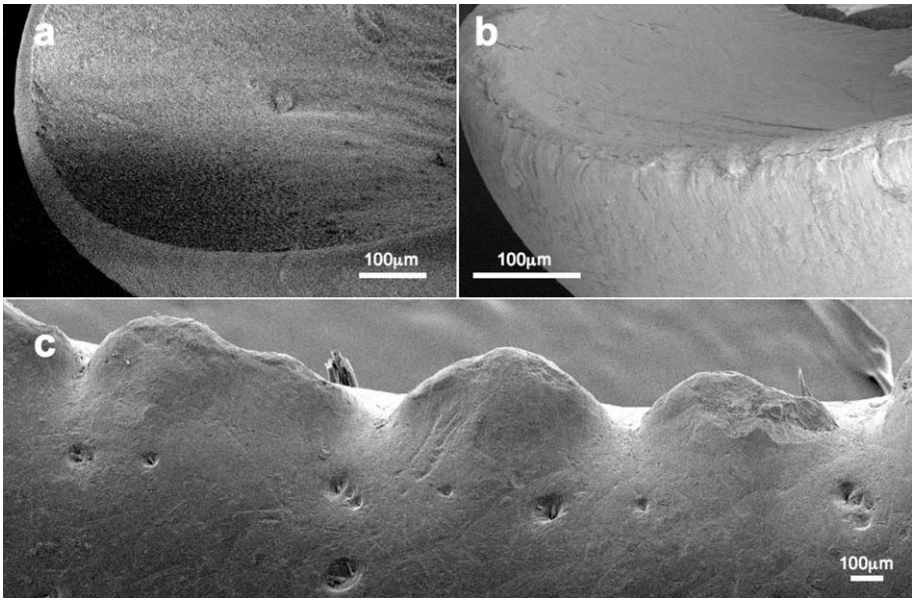

Fig. 13. Damage patterns in the bromine-rich spoon tips and calcified claw teeth of the chelipeds of *P. crassipes*. SEM images a and b are of spoon tips of newly molted (a) and older (b) crabs. Image c is of the same claw as b, but shows the teeth of the calcified region of the claw. Fractures have reshaped the calcified teeth (c), but not the profile of the spoon tip (b). Most of the cracks visible in the spoon tip have not removed material and are likely to be associated with drying for SEM. The 7 nm laminae of the spoon tips radiate from the center of the spoon, which insures that fracture planes between laminae (which require only 0.67 as much energy as fractures across the laminae) would split the edge, but not break off the lip of the spoon. Wear marks in b appear to follow the laminae. Mechanical property measurements were made on the surface (except for energy of fracture), edge-on to the laminae.

cies as the damped vibrations (Boyd, 1985a,b; Wert, 1986). The attachment of many heavy bromine atoms to many phenyl rings along the protein would reduce the resonant frequencies of certain low frequency large-scale molecular motions (such as standing torsional waves over the length of the molecule). If these resonances were lowered to overlap more with the range of frequencies associated with impacts, then bromination might improve damping of impact energy.

4. Summary

(1) The spoon-like cheliped tips of the crab *P. crassipes* are not calcified like the rest of the claw but instead contain bromine in concentrations reaching about 1% of dry mass. The tips also contain chitin and at least 35% protein.

(2) The bromine-rich spoon tips are characterized by 7 nm-spaced laminae and 5 μm-scale tubes (which may be conduits for chemoreception), both oriented perpendicular to the cuticle surface. The laminae and tubes are oriented so that a fracture plane that severs the tip would cross the laminae and tubes rather than run parallel to the interfaces, and would require a factor of 1.5 more energy per unit area of fracture. The 7 nm scale is 1/1000 of the scale of crystals in calcified cuticle, making possible tips or edges that are sharp on a micron scale and smaller.

(3) The bromine EXAFS spectra of spoon tips are similar to spectra for models and standards of brominated phenyl rings, are less similar to spectra for brominated histidine, and dibrominated phenyl rings, and are quite different from bromine EXAFS of an aliphatic bromine compound. The atomic structure within about a nanometer of the bromine atoms is similar no matter where on the spoon tip the bromine is located.

(4) The percentage of amino acids that were tyrosine (which contains a phenyl ring) was about 10 times greater in the cheliped tips (about 5%) than in the calcified region. There was roughly one bromine atom for every two tyrosine residues in the tip.

(5) The bromine EXAFS spectra for *P. crasssipes* spoon tips were similar to spectra from the tarsal claw tips of another shore crab species, and similar to the spectra from bromine-enriched mechanical structures of several other invertebrates: Nereid worms, a pycnogonid, and a priapulid. Our results, together with previous results, indicate that many invertebrates employ singly brominated phenyl rings in mechanical structures.

(6) The bromine-rich claw cuticle was about equal to the calcified cuticle in resistance to our abrasion test; it was ~1/3 as hard as the calcified cuticle, and its modulus of elasticity was ~1/5 as great. On the other hand, the energy required to produce a fracture of unit area was ~9 times greater for the bromine-rich than for the calcified material. Relative to non-enriched cuticle from ant mandibles, the bromine-enriched cuticle was about equal in energy of fracture, but was ~1.5 times as hard and had a 1.5 times greater modulus of elasticity.

(7) For sinusoidal indentations at 10 Hz, we found that the rate of energy loss was several times greater for brominated cuticle than for calcified cuticle. Eighty-six percent of the energy stored in vibrating structures of brominated cuticle would be lost in only 2.5 cycles. While we did not directly test dynamic mechanical properties at the much higher frequencies associated with impact, we did qualitatively demonstrate that the brominated cuticle was more resistant to impacts from bead blasting.

(8) The greater viscoelasticity and plasticity of the brominated cuticle should further enhance fracture resistance because some energy is diverted into rearranging molecules and so may not be available for fracture. Brominated cuticle can withstand a greater deformation before fracture for slower interactions.

(9) Our results suggest that the main advantage of brominated cuticle over calcified cuticle is resistance to fracture. Other things being equal, a spoon tip made of brominated instead of calcified cuticle would require a 6 times greater deflection, and a 1.4–3 times greater force to produce the same area of fracture. The main advantage of brominated cuticle over unenriched cuticle is that it has a higher modulus of elasticity and hardness (though not as high as for calcified cuticle). Our data suggest no advantage in

using brominated cuticle in regions susceptible to abrasion, that an exoskeleton of brominated rather than calcified cuticle could resist a factor of 1.4 greater force before rupture during attack, that calcified cuticle would be best for regions designed to apply large pressures, but that were not sensitive to fracture, and that the brominated cuticle would be optimal for sharp edges and tips that must keep their shape under pressure and not fracture.

(10) A comparison with other natural and man-made materials indicated that the brominated cuticle was harder and stiffer than the hardest tested plastic, acrylic (PMMA). Unenriched mandible cuticle was about the same hardness as acrylic. Brominated cuticle was comparable to acrylic in low frequency dynamic mechanical properties. Salmon tooth was harder but less fracture resistant than brominated cuticle, and cat claw was more fracture resistant but not as hard.

(11) We hypothesize that smaller organisms would be more likely to trade hardness and stiffness for fracture resistance, based on the importance of fracture resistance in regions of small cross-sectional area. We hypothesize that small organisms will tend to employ sharp tips and edges slowly, when possible, to take advantage of viscoelasticity and to reduce uncontrolled forces that can lead to fracture.

(12) One possible function of bromine is to harden and stiffen by increasing cross-links. We also speculate that bromine and other heavy elements employed in heavy-element biological materials may improve absorption of energy from impacts by virtue of their high mass density, lowering the resonant frequencies of low-frequency molecular motions to give more overlap with the range of vibration frequencies produced by impacts.

Acknowledgments

We would like to thank V. Storch for providing priapulid specimens. K. Emmett, J. St. John, M. Barnett, K. Hogan, A. Beiderwell, M. Richardson, F. Tyler, W. Teichman, E. D'Ambrosio and B. Bakalarova helped with collection and care of specimens. This work was supported by NSF Grant IOS 0422234. Portions of this research were carried out at the Stanford Synchrotron Radiation Lightsource, a national user facility operated by Stanford University on behalf of the US Department of Energy, Office of Basic Energy Sciences. The SSRL Structural Molecular Biology Program is supported by the Department of Energy, Office of Biological and Environmental Research, and by the National Institutes of Health, National Center for Research Resources, Biomedical Technology Program.

References

Ashby, M.F., Gibson, L.J., Wegst, U., Olive, R., 1995. The mechanical properties of natural materials. I. Material property charts. Proceedings of the Royal Society of London A 450, 123–140.

Barber, S.B., 1961. Chemoreception and thermoreception. In: Waterman, T.H. (Ed.), The Physiology of Crustacea, Volume II Sense Organs, Integration, and Behavior. Academic Press, New York.

Behrens Yamada, S., Boulding, E.G., 1998. Claw morphology, prey size selection and foraging efficiency in generalist and specialist shell-breaking crabs. Journal of Experimental Marine Biology and Ecology 220, 191–211.

Birkedal, H., Rashda, K., Khan, R.K., Slack, N., Broomell, B., Lichtenegger, H.C., Zok, F., Stucky, G.D., Waite, J.H., 2006. Halogenated veneers: protein cross-linking and halogenation in the jaws of Nereis, a marine polychaete worm. ChemBioChem 7, 1392–1399.

Boyd, R.H., 1985a. Relaxation processes in crystalline polymers: experimental behaviour—a review. Polymer 26, 323–347.

Boyd, R.H., 1985b. Relaxation processes in crystalline polymers: molecular interpretation—a review. Polymer 26, 1123–1133.

Broomell, C.C., Mattoni, M.A., Zok, F.W., Waite, J.H., 2006. Critical role of zinc in hardening of *Nereis* jaws. The Journal of Experimental Biology 209, 3219–3225.

Bovbjerg, R.V., 1960. Behavioral ecology of the crab, *Pachygrapsus crassipes*. Ecology 41, 668–672.

Bryan, G.W., Gibbs, P.E., 1979. Zinc—a major inorganic component of nereid polychate jaws. Journal of the Marine Biological Association of the UK 59, 969–973.

Ferry, J.D., 1980. Viscoelastic Properties of Polymers. John Wiley & Sons, New York.

Giddings, V.L., Kurtz, S.M., Jewett, C.W., Foulds, J.R., Edidin, A.A., 2001. A small punch test technique for characterizing the elastic modulus and fracture behavior of PMMA bone cement used in total joint replacement. Biomaterials 22, 1875–1881.

Goldberg, W.M., Hopkins, T.L., Holl, S.M., Schaefer, J., Kramer, K.J., Morgan, T.D., Kim, K., 1994. Chemical composition of the sclerotized black coral skeleton (Coelenterata: Antipatharia): a comparison of two species. Comparative Biochemistry and Physiology B 107, 633–643.

Hsiao, Y.W., Tao, Y., Shokes, J.E., Scott, R.A., Ryde, U., 2006. EXAFS structure refinement supplemented by computational chemistry. Physical Review B 74, 214101-1–214101-17.

Hunt, S., Breuer, S.W., 1971. Description of a new naturally occuring halogenated amino acid: monochloromonobromotyrosine. Biochimica et Biophysica Acta 252, 401–404.

Ishiyama, C., Higo, Y., 2002. Effects of humidity on Young's modulus in poly(methyl methacrylate). Journal of Polymer Science. Part B: Polymer Physics 40, 460–465.

Juanes, F., Hartwick, E.B., 1990. Prey size selection in Dungeness crabs: the effect of claw damage. Ecology 71, 744–758.

Lakes, R.S., 1998. Viscoelastic Solids. CRC Press, New York.

Low, E.M., 1951. Halogenated amino acids of the bath sponge. Journal of Marine Research 10, 239–245.

Lupton, R., 1993. Statistics in Theory and Practice. Princeton University Press, Princeton, NJ.

Main, I.G., 1978. Vibrations and Waves in Physics. Cambridge University Press, Cambridge, United Kingdom.

Melnick, C.A., Chen, Z., Mecholsky, J.J., 1996. Hardness and toughness of exoskeleton material in the stone crab, *Menippe mercenaria*. Journal of Materials Research 11, 2903–2907.

Minke, R., Blackwell, J., 1978. The structure of α-chitin. Journal of Molecular Biology 120, 167–181.

Oliver, W.C., Pharr, G.M., 2004. Measurement of hardness and elastic modulus by instrumented indentation: advances in understanding and refinements to methodology. Journal of Materials Research 19, 3–20.

Oliver, W.C., Pharr, G.M., 1992. An improved technique for determining hardness and elastic modulus using load and displacement sensing indentation experiments. Journal of Materials Research 6, 1564–1583.

Palmer, A.R., Taylor, G.M., Barton, A., 1999. Cuticle Strength and the size-dependence of safety factors in *Cancer* crab claws. Biol. Bull. 196, 281–294.

Pickering, I.J., Hirsch, G., Prince, R.C., Yu Sneeden, E., Salt, D.E., George, G.N.J., 2003. Imaging of selenium in plants using tapered metal monocapillary optics. Journal of Synchrotron Radiation 10, 289–290.

Pontin, M.G., Moses, D.N., Waite, J.H., Zok, F.W., 2007. A nonmineralized approach to abrasion resistant biomaterials. Proceedings of the National Academy of Sciences 104, 13559–13564.

Pryor, M.G.M., 1962. Sclerotization. In: Florkin, M., Mason, H.S. (Eds.), Constituents of Life—Part B (IV), Comparative Biochemistry. Academic Press, New York.

Rappe, A.K., Casewit, C.J., Colwell, K.S., Goddard, W.A., Skid, W.M., 1992. UFF, a full periodic table force field for molecular mechanics and molecular dynamics simulations. Journal of the American Chemical Society 114, 10024–10035.

Ricketts, E.F., Calvin, J., Hedgpeth, J.W., Phillips, D.W., 1985. Between Pacific Tides, fifth ed. Stanford University Press, Stanford, CA.

Roche, J., 1952. Biochimie comparee des scleroproteines iodees des Anthozoaires et des Spongiaires. Experientia 8, 45–84.

Roer, R.D., Dillaman, R.M., 1993. Molt-related changes in integumental structure and function. In: Horst, M.N., Freeman, J.A. (Eds.), The Crustacean Integument. CRC Press, Boca Raton.

Schofield, R.M.S., 1990. X-ray microanalytic concentration measurements in unsectioned specimens: a technique and its application to Zn, Mn, and Fe enriched mechanical structures of organisms from three phyla. Ph.D. Dissertation, University of Oregon, 185 pp.

Schofield, R.M.S., 2001. Metals in cuticular structures. In: Brownell, P., Polis, G. (Eds.), Scorpion Biology and Research. Oxford University Press, Oxford.

Schofield, R.M.S., Lefevre, H.W., 1993. Analysis of unsectioned specimens: 2D and tomographic PIXE with STIM. Nuclear Instruments and Methods in Physics Research B 77, 217–224.

Schofield, R.M.S., Nesson, M.H., Richardson, K.A., 2002. Tooth hardness increases with zinc-content in mandibles of young adult leaf-cutter ants. Naturwissenschaften 89, 579–583.

Schofield, R.M.S., Nesson, M.H., Richardson, K.A., 2003. Zinc is incorporated into cuticular "tools" after ecdysis: the time course of zinc accumulation in "tools" and whole bodies of an ant and a scorpion. Journal of Insect Physiology 49, 31–44.

Seed, R., Hughes, R.N., 1995. Criteria for prey size-selection in molluscivorous crabs with contrasting claw morphologies. Journal of Experimental Marine Biology and Ecology 193, 177–195.

Smallegange, I.M., Van Der Meer, J., 2003. Why do shore crabs not prefer the most profitable mussels? Journal of Animal Ecology 72, 599–607.

Steinbrecht, R.A., Stankiewicz, B.A., 1999. Molecular composition of the wall of insect olfactory sensilla—the chitin question. Journal of Insect Physiology 45, 785–790.

Tao, Y., Shokes, J.E., Scott, R.A., Nesson, M.H., Schofield, R.M.S., 2007. XAFS studies of transition metal and halogen biomaterials in invertebrate tools. In: AIP Conference Proceedings, vol. 882, pp. 352–354.

Taylor, G.M., 2001. The evolution of armament strength: evidence for a constraint on the biting performance of claws of durophagous decapods. Evolution 55, 550–560.
Taylor, G.M., Palmer, A.R., Barton, A.C., 2000. Variation in safety factors of claw with and among six species of *Cancer* crabs (Decapoda: Brachyura). Biological Journal of the Linnean Society 70, 37–62.
Vincent, J.F.V., 1982. Structural Biomaterials. John Wiley & Sons, New York.
Vogel, S., 2003. Comparative Biomechanics. Princeton University Press, Princeton, NJ.
Warner, G.F., 1977. The Biology of Crabs. Van Nostrand Reinhold Co., New York.
Welinder, B.S., 1972. Halogenated tyrosines from the cuticle of *Limulus polyphemus* (L.). Biochimica et Biophysica Acta 279, 491–497.
Wert, C.A., 1986. Internal friction in solids. Journal of Applied Physics 60, 1888–1895.